*J. Fluid Mech.* (1992), *vol.* 244, *pp.* 241–256



# The characteristics of laminar flow in a helical circular pipe

By WEN-HWA CHEN AND RAY JAN

Department of Power Mechanical Engineering, National Tsing Hua University, Hsinchu, Taiwan 30043, ROC

(Received 8 November 1991 and in revised form 13 March 1992)

The fully developed laminar flow in a helical circular pipe under the influence of both curvature and torsion is studied analytically. The solutions are obtained by the double series expansion method which perturbs the exact solution derived in this work for a twisted circular pipe. The perturbed parameters selected are dimensionless curvature $\kappa$ and dimensionless torsion $\tau$. Since the expanded governing equations and series solutions have been arranged in a compact form, the complete solutions can be computed by a systematic procedure on computer. In addition, the accuracy of the solutions is only confined by the natural limitation of the series expansion method because no approximation was made in the governing equations. The 'torsion number' $Tn$ which can be considered as the measure of the torsion effect that swirls the flow is defined $Tn = 2\tau\mathscr{R}$, where $\mathscr{R}$ is the Reynolds number. The characteristics of the flow in the helical circular pipe are thus controlled by three parameters: $\mathscr{R}$, Dean number $K$ and $Tn$. The flow rate solution of the extended Dean equations of Germano (1989) is then found. The effects of finite curvature and torsion on the flow rate, axial velocity and secondary flow are also found. The inconsistency of torsion effect on the secondary flow between Wang (1981) and Germano (1982, 1989) is also quantitatively explained by the different coordinate systems used.

## 1. Introduction

Helical pipes are used extensively in various industrial applications, especially in cooling or heating devices. Owing to the secondary flow generated by the centrifugal force and twisting force, the rates of heat, mass and momentum transfer in helical pipes are usually much different from those in straight or toroidal pipes. Hence, the study of flows in helical pipes deserve attention.

In the literature, most of the theoretical studies have been concentrated on toroidal pipes without pitch (Berger, Talbot & Yao 1983; Ito 1987). Studies on the flow in helical pipes are relatively limited (Manlapaz & Churchill 1980; Wang 1981; Murata *et al.* 1981; Germano 1982, 1989; Chen & Fan 1986; Kao 1987; Xie 1990; Tuttle 1990). In those previous studies, it is concluded that the behaviour of the flow in a helical pipe can be approximated by that in a toroidal pipe if the pitch or torsion is small. However, inconsistent conclusions have been drawn for flow rate and secondary flow.

Manlapaz & Churchill (1980) made a numerical calculation of the flow rate, in a helically coiled tube of finite pitch over the whole laminar flow region. They obtained an equation for determining the friction factor and concluded that the pitch effect is insignificant only for coils for which the increase in elevation per revolution of coils is less than the radius of the coil. However, one of the present authors (Chen & Fan

1986) derived the governing equations for the flow in a helical pipe with finite curvature and torsion using the non-orthogonal coordinate system as used by Wang (1981) and showed that the torsion effect on the flow rate can be ignored. Kao (1987) also concluded that the torsion effect is always small in all the circumstances of his results. This inconsistency reveals that both pitch and torsion, although they are usually adopted to describe the geometry of helical pipes, seem to be inappropriate to characterize the torsion effect on the flow rate. Considering loosely coiled pipes, Germano (1989) showed that the flow in a helical circular pipe depends not only on the Dean number $K$ but also on a new parameter $\lambda/\mathscr{R}$, where $\lambda$ is the ratio of the torsion $\tau$ to the curvature $\kappa$ of the centreline of the pipe and $\mathscr{R}$ is the Reynolds number. The dimensionless $\tau$ and $\kappa$ are normalized by the radius $a$ of the pipe. This new parameter is obtained from the derivation of the compact governing equations which are an extension of the Dean equations (Dean 1928) and is more conceptually useful to describe the flow in the helical pipe. However, the analysis is valid only for cases with small curvature and small torsion.

One of the objectives of this work is thus to pursue a new dimensionless parameter, the 'torsion number' $Tn$, which can be used as an estimation of the torsion effect on the flow in the helical pipe and is defined as $2\tau\mathscr{R}$. Since the high-order terms of curvature and torsion are considered, unlike previous studies (Germano 1982, 1989; Kao 1987) the solutions obtained from the general governing equations by the double series expansion method are applicable to a wider range of curvature and torsion. The results show that the flow in a helical pipe is controlled by three parameters: Reynolds number $\mathscr{R}$, Dean number $K$ and torsion number $Tn$.

For the secondary flow, the results of the torsion effect obtained by Wang (1981) and by Germano (1982) are different. Using a non-orthogonal coordinate system, Wang (1981) mentioned that both curvature and torsion play important roles in the flow and the torsion can be so dominant in some phenomena, for example, to even change a two-vortex secondary flow to a single vortex one. Introducing a transformation and rendering the governing equations for a helical circular pipe expressible in an orthogonal coordinate system, Germano (1982) showed that only the curvature can cause a first-order effect and the torsion effect is of second order. Kao (1987) used the Germano's orthogonal coordinate system, and tried to settle these differences using series expansion and numerical methods. He indicated that the torsion produces a significant influence on the secondary flow pattern if the ratio of curvature to torsion is of order unity and in general the torsion effect is small, and the secondary flow usually has a two-vortex pattern. However, the mechanism of the torsion effect is still not clear. With a detailed comparison between the non-orthogonal and orthogonal coordinates of Wang (1981) and Germano (1982), respectively, Tuttle (1990) qualitatively stated that the order of the torsion effect on the secondary flow depends on the frame of reference of the observer. For the secondary flow represented by the Dean's recirculating cells which are observed on the non-orthogonal coordinate system, Tuttle (1990) concluded that the torsion has a first-order effect. To give a more clear explanation of the torsion effect on the secondary flow, an exact solution of the governing equations established in the non-orthogonal coordinate system for a twisted circular pipe is also derived in this work.

As in the study of Tuttle (1990), the present solutions are also expanded in a power series not only of dimensionless curvature $\kappa$ but also of dimensionless torsion $\tau$. The primary solutions derived from the exact solution of the twisted circular pipe, as mentioned, after an appropriate transformation, can be shown the same as those of Tuttle (1990). The expanded governing equations and series solutions are rearranged

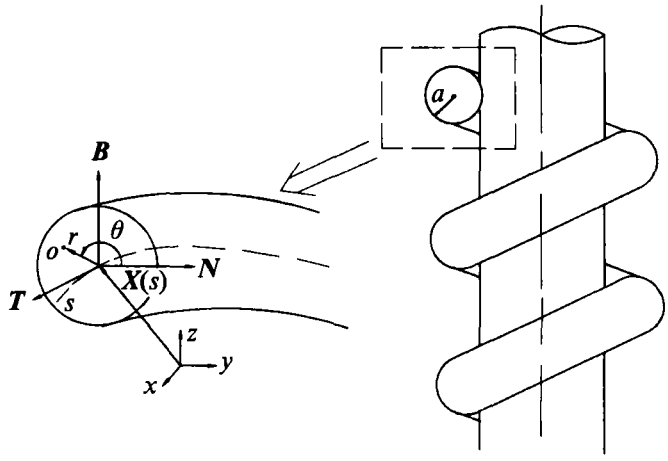


FIGURE 1. Non-orthogonal helical coordinate system.

in a compact form, which allows the axial velocity and stream function to be computed with a systematic procedure. With these solutions, the effects of finite curvature and finite torsion on the flow rate, axial velocity and secondary flow in a helical circular pipe can thus be realized clearly.

## 2. Coordinate system and governing equations

To derive the governing equations the non-orthogonal helical coordinate system as used by Wang (1981), shown in figure 1, is again adopted. The centreline of the helical circular pipe is described by the position vector $\boldsymbol{X}(s)$, where $s$ represents the dimensionless arclength normalized by the radius of the helical pipe $a$. Along the centreline, the unit tangent, normal and binormal vectors are mutually orthogonal and denoted by $\boldsymbol{T}$, $\boldsymbol{N}$ and $\boldsymbol{B}$, respectively. Hence, an arbitrary point $o$ can be expressed by the helical coordinate system $(r, \theta, s)$ which is constructed with the coordinates $(r, \theta)$ defined by the plane of $\boldsymbol{N}$ and $\boldsymbol{B}$ and the normalized arclength $s$ is taken as the third coordinate along the axial direction of the centreline of the helical pipe. The radial distance $r$ is measured from the centreline and the angle $\theta$ is measured from the normal $\boldsymbol{N}$ in a counterclockwise direction. $r$ is also normalized by the radius of the pipe $a$.

Although the $r$- and $s$-coordinates and $r$- and $\theta$-coordinates are mutually orthogonal, the $\theta$- and $s$-coordinates are non-orthogonal except at the centreline of the pipe where the direction of $s$ coincides with tangential vector $\boldsymbol{T}$. Detailed discussion of the orthogonal and non-orthogonal helical coordinate system can be found in Chen & Fan (1986).

Introduce the dimensionless velocity components $u$, $v$ and $w$ and dimensionless pressure $p$ as

$$u = \frac{a}{\nu}U, \quad v = \frac{a}{\nu}V, \quad w = \frac{a}{\nu}W, \quad p = \frac{P}{\rho}\left(\frac{a}{\nu}\right)^2,$$

where $U$, $V$ and $W$ represent the physical velocity components in the $r$-, $\theta$- and $s$-directions, $P$ is the pressure, $\nu$ is the kinematic viscosity and $\rho$ is the density.

For steady, incompressible, fully developed laminar flow, $(\partial/\partial s)(u, v, w)$ vanishes, and $(u, v, w)$ and $p$ are independent of time. Furthermore, the axial pressure gradient $\partial p/\partial s$ is a given constant. Based on these, the governing equations are as follows (Chen & Fan 1986).

(i) *Continuity equation*

$$\frac{\partial u}{\partial r}+\frac{1}{r}\frac{\partial v}{\partial \theta}+\frac{u}{r}+\frac{\kappa}{m}(v\sin\theta-u\cos\theta)=0; \tag{1}$$

(ii) *Navier–Stokes equations*

in the $r$-direction

$$u\frac{\partial u}{\partial r}+\frac{v}{r}\frac{\partial u}{\partial \theta}-\frac{v^2}{r}-\frac{2\tau}{h}vw-(\tau^2 r-\kappa m\cos\theta)\left(\frac{w}{h}\right)^2=-\frac{\partial p}{\partial r}+\nabla^2 u-\frac{2}{r^2}\frac{\partial v}{\partial \theta}-\frac{2\tau}{hmr}\frac{\partial w}{\partial \theta}$$
$$-\left(\frac{1}{r^2}+\left(\frac{\kappa\cos\theta}{m}\right)^2\right)u-\left(\frac{\kappa\sin\theta}{rm}-\frac{\kappa^2\cos\theta\sin\theta}{m^2}\right)v+\frac{2\kappa\tau\sin\theta}{h^3}w; \tag{2}$$

in the $\theta$-direction

$$u\frac{\partial v}{\partial r}+\frac{v}{r}\frac{\partial v}{\partial \theta}+\frac{vu}{r}-\frac{\kappa\sin\theta}{m}w^2+\frac{2\tau}{hm}(u-v\kappa r\sin\theta)w=$$
$$-\frac{h^2}{rm^2}\frac{\partial p}{\partial \theta}+\frac{\tau r}{m^2}\frac{\partial p}{\partial s}+\nabla^2 v+\left(\frac{2}{r^2}-\frac{2\kappa\tau^2 r\cos\theta}{m^3}\right)\frac{\partial u}{\partial \theta}$$
$$+\frac{2\kappa\tau^2 r\sin\theta}{m^3}\frac{\partial v}{\partial \theta}+\frac{2\tau}{hm}\frac{\partial w}{\partial r}+\frac{h^2\kappa\sin\theta}{rm^4}u-\left(\frac{1}{r^2 m}-\frac{h^2\kappa\cos\theta}{rm^4}+\left(\frac{\kappa h}{m^2}\right)^2\right)v+\frac{2\tau}{h^3}\left(\kappa\cos\theta-\frac{\tau^2 r}{m}\right)w; \tag{3}$$

in the $s$-direction

$$u\frac{\partial w}{\partial r}+\frac{v}{r}\frac{\partial w}{\partial \theta}+\frac{\kappa}{m}(v\sin\theta-u\cos\theta)w+\frac{\kappa\tau r\sin\theta}{hm}w^2-\frac{r\tau^2}{h^2 m}(u-v\kappa r\sin\theta)w=$$
$$+\frac{h}{m^2}\left(-\frac{\partial p}{\partial s}+\tau\frac{\partial p}{\partial \theta}\right)+\nabla^2 w+\frac{2\kappa\tau h}{m^3}\left(\frac{\partial u}{\partial \theta}\cos\theta-\frac{\partial v}{\partial \theta}\sin\theta\right)$$
$$-\frac{2\tau^2 r}{mh^2}\frac{\partial w}{\partial r}+\frac{\kappa\tau h}{m^4}(v\kappa r-v\cos\theta-u\sin\theta)-\left(\frac{\kappa^2}{h^2}+\frac{\tau^2}{h^2}\left(1-\frac{2}{m}+\frac{3}{h^2}\right)\right)w; \tag{4}$$

where $$\nabla^2=\frac{\partial^2}{\partial r^2}+\left(\frac{1}{r}-\frac{\kappa\cos\theta}{m}\right)\frac{\partial}{\partial r}+\left(\frac{\kappa\sin\theta}{mr}-\frac{\kappa\tau^2 r\sin\theta}{m^3}\right)\frac{\partial}{\partial \theta}+\left(\frac{h}{rm}\right)^2\frac{\partial^2}{\partial\theta^2},$$
$$h^2=m^2+\tau^2 r^2,\quad m=1-\kappa r\cos\theta.$$

Since the stream functions used in the literature (Wang 1981; Kao 1987; Germano 1989) are all confined to the cases of small curvature and torsion, to preserve the high-order terms of torsion and curvature in the governing equations, the stream function $\psi$ that satisfies the continuity equation without any simplification is redefined here as follows:

$$u=\frac{1}{rm}\frac{\partial\psi}{\partial\theta},\quad v=-\frac{1}{m}\frac{\partial\psi}{\partial r}. \tag{5}$$

Substituting the stream function for $(u, v)$ as stated in (5) into (2)–(4) and eliminating the pressure terms ($\partial p/\partial r$ and $\partial p/\partial\theta$) between (2) and (3) and (3) and (4), one obtains the following set of equations which are written in terms of the unknowns $w_h$ and $\psi$:

$$\nabla^4\psi+\frac{1}{mr}\frac{\partial(\psi,\nabla^2\psi)}{\partial(r,\theta)}-2\tau\left(\nabla^2 w_h+\frac{1}{h^2}\frac{\partial p}{\partial s}\right)=$$
$$2h^2 w_h\left(\kappa\sin\theta\frac{\partial w_h}{\partial r}+\frac{m-h^2}{mr^2}\frac{\partial w_h}{\partial\theta}\right)+\frac{2\tau}{mr}\left(\frac{1}{m}\frac{\partial\psi}{\partial r}\frac{\partial w_h}{\partial\theta}-\frac{\partial\psi}{\partial\theta}\frac{\partial w_h}{\partial r}\right)+\frac{F_1}{mr}, \tag{6}$$

and
$$\nabla^2 w_h + \frac{1}{mr}\frac{\partial(\psi, w_h)}{\partial(r,\theta)} - \frac{1}{h^2}\frac{\partial p}{\partial s} = \frac{F_2}{h^2}, \tag{7}$$

where
$$w_h = \frac{w}{h} \quad \text{and} \quad \frac{\partial(G,H)}{\partial(r,\theta)} = \frac{\partial G}{\partial r}\frac{\partial H}{\partial \theta} - \frac{\partial G}{\partial \theta}\frac{\partial H}{\partial r}.$$

The high-order terms for curvature and torsion are collected in the functions of $F_1$ and $F_2$.† When the curvature is small, the functions $F_1$ and $F_2$ can be neglected because their orders are higher than $O(\kappa^0)$ and $O(\kappa^{-\frac{1}{2}})$ of the terms in (6) and (7), respectively. This can be achieved by taking $\partial p/\partial s = O(\kappa^{-\frac{1}{2}})$ and $\tau = O(\kappa^{\frac{1}{2}})$. It is noted that the orders of $w_h$ and $\psi$ can be obtained from the exact solutions of the twisted pipe appearing in the following section as $w_h = O(\kappa^{-\frac{1}{2}})$ and $\psi = O(\kappa^0)$. Similar ordering arguments can be also seen in Kao (1987).

The boundary conditions are

$$w_h = 0, \quad \psi = 0, \quad \text{and} \quad \frac{\partial \psi}{\partial r} = 0 \quad \text{at} \quad r = 1. \tag{8}$$

In addition, other conditions for $w_h$ and $\psi$ are obtained from the fact that the velocity components $u$, $v$ and $w$ must be finite over the entire cross-section.

To get the solutions of (6) and (7) satisfying (8), successive approximations to the solutions can be made by expanding both $w_h$ and $\psi$ as power series in curvature and torsion. Furthermore, such successive approximations start from the exact solution of the flow in a twisted pipe instead of the Poiseuille flow. This will be described in the next section.

## 3. Exact flow solution for a twisted circular pipe

A comparison among different types of pipe is displayed in figure 2. As seen in figure 2, the helical pipe the curvature of which vanishes is named the twisted pipe. The twisted circular pipe is axisymmetric because of its circular cross-section and $u = 0$ and $\partial(u, v, w, p)/\partial\theta = 0$. The continuity equation as stated in (1) is hence automatically satisfied and the Navier–Stokes equations (2)–(4) can be simplified as follows:

in the $r$-direction
$$\frac{v^2}{r} + \frac{2\tau}{h} vw + \tau^2 r\left(\frac{w}{h}\right)^2 = 0; \tag{9}$$

in the $\theta$-direction
$$\frac{\partial^2 v}{\partial r^2} + \frac{1}{r}\frac{\partial v}{\partial r} + \frac{2\tau}{h}\frac{\partial w}{\partial r} - \frac{v}{r^2} - \frac{2\tau^3 r}{h^3} w = -\tau r \frac{\partial p}{\partial s}; \tag{10}$$

in the $s$-direction
$$\frac{\partial^2 w}{\partial r^2} + \frac{1}{r}\frac{\partial w}{\partial r} - \frac{2\tau^2 r}{h^2}\frac{\partial w}{\partial r} - \frac{\tau^2}{h^2}\left(\frac{3}{h^2} - 1\right) w = h\frac{\partial p}{\partial s}. \tag{11}$$

It is difficult to solve these simultaneous partial differential equations (9)–(11) directly. However, the solutions under the present non-orthogonal helical coordinate system can be obtained by a suitable transformation from those available for straight pipes. The results are

$$v = \frac{\tau r}{4}\frac{\partial p}{\partial s}(1 - r^2), \tag{12}$$

† The details of the functions $F_1$ and $F_2$ can be requested from the authors, or the Journal of Fluid Mechanics Editorial Office.

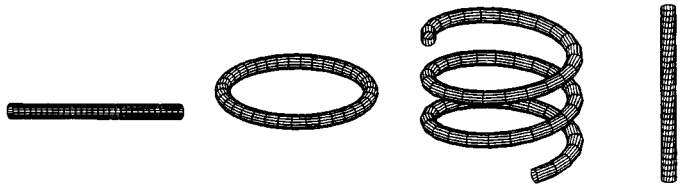

| $\tau = 0$ | $\tau = 0$ | $\tau = 0.01$ | $\tau = 0.1$ |
|---|---|---|---|
| $\kappa = 0$ | $\kappa = 0.1$ | $\kappa = 0.1$ | $\kappa = 0$ |
| Straight pipe | Toroidal pipe | Helical pipe | Twisted pipe |

FIGURE 2. Comparison among different types of pipe.

and
$$w = -\frac{1}{4}\frac{\partial p}{\partial s}(1+\tau^2 r^2)^{\frac{1}{2}}(1-r^2). \tag{13}$$

The stream function for this case can be further expressed as

$$\psi = \frac{\tau}{16}\frac{\partial p}{\partial s}(1-r^2)^2. \tag{14}$$

As seen in figure 2, the twisted circular pipe can be obtained by twisting the wall of a straight circular pipe. Owing to the circular cross-section, there is no warping of the cross-section and the shapes of these twisted and straight pipes are the same. Hence, the flow in a twisted circular pipe is exactly the same as that in a straight pipe, for which no secondary flow is found in the laminar flow region. As a result, no torsion effect on the secondary flow can be observed for the twisted circular pipe. However, for a twisted pipe with different cross-sections, the above conclusion should be modified. As shown by previous studies (Todd 1977; Kotorynski 1986; Germano 1989; Tuttle 1990), torsion has a first-order effect on the secondary flow for a twisted pipe with elliptical cross-section.

The stream function in (14) denotes the rotation motion produced by the term $\tau r\,\partial p/\partial s$ as stated in (10). This can be seen because of the use of the present non-orthogonal coordinate system. Although the twisting force produced in the twisted circular pipe due to the non-orthogonal helical coordinate system is only a virtual one, it is expected that the influence of this force will exist in the helical pipe. For a twisted pipe with a cross-section which is not axisymmetric (Germano 1989), the torsional rotation of the wall of the pipe pushes the flow and that is also an essential element of the twisting force.

## 4. Double series expansion solution for a helical circular pipe

To obtain the flow solution for a helical circular pipe, the double series expansion method is adopted in this work. The series solutions are expanded in both dimensionless curvature $\kappa$ and dimensionless torsion $\tau$. The successive approximation can be obtained based on the solution of twisted circular pipe as derived in the previous section. In order to preserve the high-order terms of curvature and torsion appearing in the governing equations (6) and (7), tedious successive approximations need to be done. Accordingly, with the aid of symbolic manipulation on a computer, the solution of the dimensionless axial velocity $w_h$ and the stream function $\psi$ for the helical circular pipe can be assumed in a series form:

$$w_h = w_{00} + \sum_{i=1,j=0}^{\infty} \kappa^i \tau^j w_{ij}, \quad \psi = \tau\psi_{00} + \sum_{i=1,j=0}^{\infty} \kappa^i \tau^j \psi_{ij}, \tag{15}$$

where the primary solutions $w_{00}$ and $\psi_{00}$, which are found as those of Tuttle (1990), can be determined from the exact solution of the twisted circular pipes as stated in (13) and (14) ($w_{0j} = \psi_{0j} = 0$ for $j \neq 0$), say,

$$w_{00} = -\frac{1}{4}\frac{\partial p}{\partial s}(1-r^2), \quad \psi_{00} = \frac{1}{16}\frac{\partial p}{\partial s}(1-r^2)^2. \tag{16}$$

Substituting (15) into (6) and (7) and collecting the terms of equal orders, one has

$$\begin{aligned}\nabla^4\psi_{ij} = {} & 2\nabla^2 w_{i(j-1)} + \frac{\partial p}{\partial s}\frac{\partial \psi_{i(j-1)}}{\partial \theta} - \frac{1}{r}\frac{\partial \psi_{00}}{\partial r}\frac{\partial \nabla^2\psi_{i(j-1)}}{\partial \theta} - \frac{1}{r}\sum_{l=1}^{i-1}\sum_{k=0}^{j}\frac{\partial(\psi_{lk}, \nabla^2\psi_{(i-l)(j-k)})}{\partial(r,\theta)} \\ & + \sum_{l=0}^{i-1}\sum_{k=0}^{j}\left(\frac{\cos\theta}{r}\frac{\partial}{\partial\theta} + \sin\theta\frac{\partial}{\partial r}\right)(w_{lk}\, w_{(i-1-l)(j-k)}) + \frac{2}{r}\sum_{l=1}^{i-1}\sum_{k=0}^{j-1}\frac{\partial(\psi_{lk}, w_{(i-l)(j-1-k)})}{\partial(r,\theta)} \\ & - 2\sum_{l=1}^{i-1}\sum_{k=0}^{j-2} w_{lk}\frac{\partial w_{(i-l)(j-2-k)}}{\partial\theta} + H_{ij}^{(1)} \quad (i = 1,2,3,\ldots, j = 0,1,2,3,\ldots),\end{aligned} \tag{17}$$

and

$$\begin{aligned}\nabla^2 w_{ij} - \frac{1}{2}\frac{\partial p}{\partial s}\frac{\partial \psi_{ij}}{\partial\theta} = {} & -\frac{1}{r}\frac{\partial\psi_{00}}{\partial r}\frac{\partial w_{i(j-1)}}{\partial\theta} - \frac{1}{r}\sum_{l=1}^{i-1}\sum_{k=0}^{j}\frac{\partial(\psi_{lk}, w_{(i-l)(j-k)})}{\partial(r,\theta)} + H_{ij}^{(2)} \\ & (i = 1,2,3,\ldots, j = 0,1,2,3,\ldots),\end{aligned} \tag{18}$$

where

$$\nabla^2 = \frac{1}{r^2}\frac{\partial^2}{\partial\theta^2} + \frac{\partial^2}{\partial r^2} + \frac{1}{r}\frac{\partial}{\partial r},$$

and $H_{ij}^{(1)}$ and $H_{ij}^{(2)}$ denote the terms contributed by the high-order terms of curvature and torsion in (6) and (7). Although the detailed expressions for $H_{ij}^{(1)}$ and $H_{ij}^{(2)}$ are too complicated to give here, the contributions of those terms have been completely included in the solutions presented herein. It is noted that $w_{ij}$ and $\psi_{ij}$ vanish once the subscript indexes become negative. In addition, the solutions $w_h$ and $\psi$ should satisfy (8) at the boundary, and from (15),

$$w_{ij} = 0, \quad \psi_{ij} = 0; \quad \frac{\partial\psi_{ij}}{\partial r} = 0. \quad \text{at} \quad r = 1, \tag{19}$$

and $w_{ij}$ and the velocity components, $u$ and $v$, computed from $\psi_{ij}$ are finite over the cross-section.

The solutions of (17) and (18) satisfying boundary conditions (19), say, $w_{ij}$ and $\psi_{ij}$, can be determined by the method of separation of variables. After tedious manipulations, the general forms of $w_{ij}$ and $\psi_{ij}$ used in the procedure of separation of variables, are found as

$$w_{ij} = \left(\frac{1}{4608}\right)^i\left(\frac{1}{64}\right)^j\sum_{k=0}^{I}\sum_{l=0}^{J}\left(-\frac{\partial p}{\partial s}\right)^{n+1} E_{ijkl}\begin{Bmatrix} r^q\cos q\theta, & j \text{ even} \\ r^q\sin q\theta, & j \text{ odd}\end{Bmatrix} \quad i > 0, \quad j \geqslant 0, \tag{20}$$

and

$$\psi_{ij} = \left(\frac{1}{4608}\right)^i\left(\frac{1}{64}\right)^j\sum_{k=0}^{I}\sum_{l=0}^{J}\left(-\frac{\partial p}{\partial s}\right)^{n} G_{ijkl}\begin{Bmatrix} r^q\sin q\theta, & j \text{ even} \\ r^q\cos q\theta, & j \text{ odd}\end{Bmatrix} \quad i > 0, \quad j \geqslant 0, \tag{21}$$

where $n = 2i+j-2k$ and $q = i-2l$. $I$ and $J$ are the greatest integers less than or equal to $\frac{1}{2}j+i$ and $\frac{1}{2}i$, respectively. The functions $E_{ijkl}$ and $G_{ijkl}$ are the polynomials of the variable $r$, the coefficients for which can be determined by solving (17) and (18) under the boundary conditions (19). To calculate any additional $w_{ij}$ or $\psi_{ij}$ of the series as stated in (15), the terms on the right-hand sides of (17) and (18) can be obtained from the preceding computations. The $w_{ij}$ and $\psi_{ij}$ and $w_h$ and $\psi$ of (15) are thus solved completely.

The range of solutions studied in this work includes the following orders of curvature and torsion,

$$\kappa^1(\tau^0 \to \tau^4), \quad \kappa^2(\tau^0 \to \tau^4), \quad \kappa^3(\tau^0 \to \tau^2), \quad \kappa^4(\tau^0 \to \tau^2). \tag{22}$$

For the case when $\tau$ vanishes, the solutions ($w_{10}$, $w_{20}$, $\psi_{10}$ and $\psi_{20}$) are reduced to those for the toroidal pipe (see figure 2), which have been proved to be as those obtained by Topakoglu (1967). Tuttle (1990) also solved the flow solution in the helical circular pipe up to the order of $\kappa^2\tau^2$. It can be shown that the present solutions are the same as those of Tuttle (1990) except the solutions of order $\kappa^2\tau^2$, $w_{22}$ and $\psi_{22}$. Although the solutions can be obtained from Topakoglu (1967) and Tuttle (1990) up to the order of $\kappa^2\tau^2$, owing to the incomplete treatment in dealing with the governing equations, the solutions of $w_{22}$ and $\psi_{22}$† of Tuttle (1990) need to be revised.

The advantages of these compact forms of (17) and (18) and the series solution of (20) and (21) are obvious. Substituting (20) and (21) into the left-hand side of (17) and (18), any terms of $w_{ij}$ and $\psi_{ij}$ (and thus $w_h$ and $\psi$) can be determined by a systematic symbolic operation procedure on computer.

## 5. Results and discussion

### 5.1. *Flow rate equation*

Owing to the non-orthogonality of the coordinate system, care should be taken that the axial velocity $w$ is not in the direction perpendicular to the $(r, \theta)$-plane where the flow passes through, except at the centreline of the pipe. As shown in figure 3, the component of axial velocity $w$ which passes through this plane is $mw_h$. Thus, the volume flux through the $(r, \theta)$-plane is defined as

$$Q = \frac{1}{A}\int_A mw_h \, \mathrm{d}A, \tag{23}$$

where $A$ is the area of the $(r, \theta)$-plane of a helical circular pipe.

Using the solutions obtained from (15), the flow rate of the helical circular pipe can be obtained as

$$\begin{aligned}
\frac{Q}{Q_s} = 1 &+ \left(\frac{K}{576}\right)^2 \{-3.0575\times10^{-2} - 5.2800\times10\mathscr{R}^{-2} + 1.7280\times10^3\mathscr{R}^{-4} \\
&+ \left(\frac{Tn}{22}\right)^2 (5.6310\times10^{-3} - 3.8895\mathscr{R}^{-2} - 7.2574\times10^3\mathscr{R}^{-4} + 1.3504\times10^5\mathscr{R}^{-6}) \\
&+ \left(\frac{Tn}{22}\right)^4 (-5.8402\times10^{-4} + 1.6444\mathscr{R}^{-2} + 1.6604\times10^3\mathscr{R}^{-4} \\
&+ 5.3798\times10^5\mathscr{R}^{-6} - 3.1624\times10^6\mathscr{R}^{-8})\} \\
&+ \left(\frac{K}{576}\right)^4 \{1.1931\times10^{-2} + 2.5863\times10\mathscr{R}^{-2} + 1.4209\times10^4\mathscr{R}^{-4} \\
&- 8.1866\times10^5\mathscr{R}^{-6} - 8.7340\times10^7\mathscr{R}^{-8} \\
&+ \left(\frac{Tn}{22}\right)^2 (-6.7179\times10^{-3} - 6.2137\mathscr{R}^{-2} + 2.8824\times10^2\mathscr{R}^{-4} + 2.7359\times10^5\mathscr{R}^{-6} \\
&- 1.0013\times10^9\mathscr{R}^{-8} + 1.6507\times10^{10}\mathscr{R}^{-10})\},
\end{aligned} \tag{24}$$

† The details of $w_{22}$ and $\psi_{22}$ are available on request from the authors, or from the Journal of Fluid Mechanics Editorial Office.

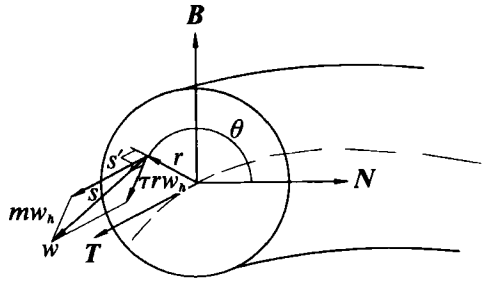


FIGURE 3. The relation between coordinate systems $(r, \theta, s)$ and $(r, \theta, s')$.

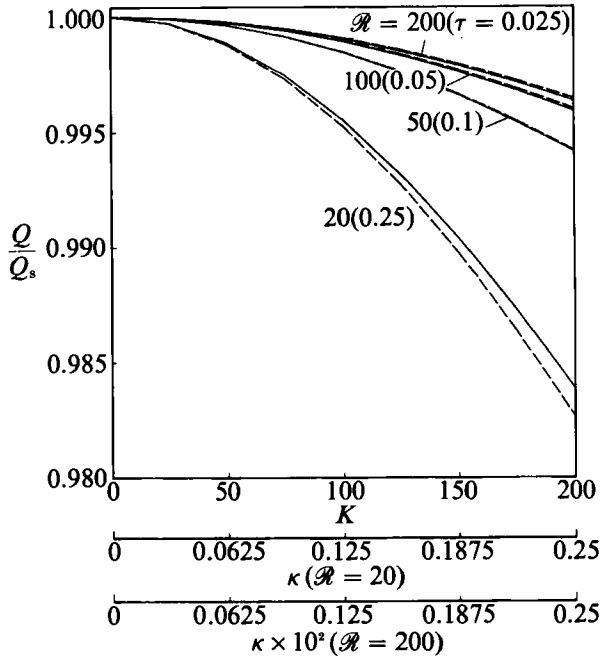


FIGURE 4. The influence of the Dean number $K$ on the flow rate: ——, $Tn = 0$ $(\tau = 0)$; – – –, $Tn = 10$.

where $Q_s$ is the volume flux of a straight pipe computed with the same axial pressure gradient $\partial p/\partial s$. The Reynolds number $\mathscr{R}$ is defined as

$$\mathscr{R} = -\frac{1}{4}\frac{\partial p}{\partial s}.$$

The Dean number $K$ and torsion number $Tn$ are

$$K = 2\kappa\mathscr{R}^2, \quad Tn = 2\tau\mathscr{R}.$$

From the solutions of the axial velocity $w_{ij}$ (20), stream function $\psi_{ij}$ (21) and flow rate equation (24), it can be concluded that the flow in a helical circular pipe is characterized by three parameters: Dean number $K$, Reynolds number $\mathscr{R}$ and torsion number $Tn$.

The influence of $\mathscr{R}$, $K$ and $Tn$ on the flow rate are depicted in figures 4 and 5, respectively. These figures can be also used to evaluate the effects of curvature $\kappa$ and torsion $\tau$ on the flow rate by appropriate adjustments. As shown in figure 4, if $Tn$ vanishes, the increase of $K$ (and hence the curvature $\kappa$) decreases the flow rate. At the

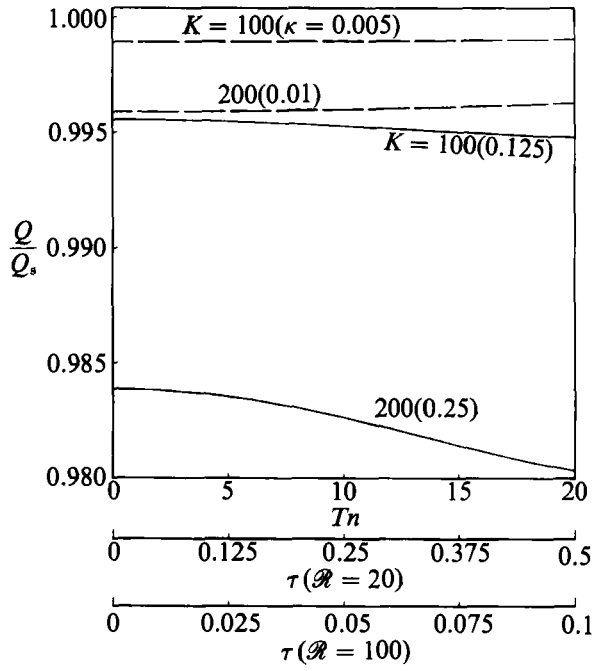


FIGURE 5. The influence of the torsion number $Tn$ on the flow rate: ——, $\mathscr{R} = 20$; – – –, $\mathscr{R} = 100$.

same value of $K$, the smaller value of $\mathscr{R}$ has a larger value of curvature $\kappa$ and therefore decreases the flow rate distinctly. In such cases, the role of high-order terms of finite curvature $\kappa$ appearing in the governing equations (2)–(4) on flow rate can be seen. The torsion effect on the flow rate is also studied for the case with $Tn = 10$. It is found that the flow rate in a helical pipe is smaller than that in toroidal pipe at small Reynolds number (with larger torsion $\tau$) while it is nearly the same at $\mathscr{R} \sim 50$. As the Reynolds number is higher than $\mathscr{R} \sim 50$, the flow rate of helical pipe behaves with a slightly reverse tendency.

The influence of the torsion number on the flow rate up to $Tn = 20$ is shown in figure 5. For smaller Reynolds number ($\mathscr{R} = 20$), the flow rate decreases as $Tn$ increases especially for the helical circular pipe with high $K$. In such cases, the effects of finite curvature and torsion are obvious. For higher Reynolds number ($\mathscr{R} = 100$), the flow rate increases slightly as $Tn$ increases. In these cases, both the curvature and torsion are relatively small and the effect of high-order terms is not so important. From (24), it is also shown that the torsion effect is enhanced as $K$ increases. For the special case of curvature $\kappa = 0$ (i.e. the Dean number vanishes), the torsion has no effect on the flow rate because the helical circular pipe is now a straight twisted pipe.

By careful comparison among the terms in (24), those with $\mathscr{R}^{-2}$, $\mathscr{R}^{-4}$, $\mathscr{R}^{-6}$, $\mathscr{R}^{-8}$ and $\mathscr{R}^{-10}$ have distinct effect on the flow rate only when the Reynolds number $\mathscr{R}$ is small. When $\mathscr{R} > 200$, however, the flow rate is mainly made up of the terms without multiplying any minus power of $\mathscr{R}$ and (24) can be simplified as

$$\frac{Q}{Q_s} = 1 + \left(\frac{K}{576}\right)^2 \left[ -3.0575 \times 10^{-2} + 5.6310 \times 10^{-3} \left(\frac{Tn}{22}\right)^2 - 5.8402 \times 10^{-4} \left(\frac{Tn}{22}\right)^4 \right] + \left(\frac{K}{576}\right)^4 \left[ 1.1931 \times 10^{-2} - 6.7179 \times 10^{-3} \left(\frac{Tn}{22}\right)^2 \right]. \quad (25)$$

As $Tn$ vanishes, (25) can be further expressed as the flow rate solution for toroidal pipes, which is the same as that obtained by Dean (1928). Also, as suggested by Van Dyke (1978) with a graphical ratio test, the Dean's flow rate series for toroidal pipes is convergent up to the Dean number $K \approx 586$. That is, the region of validity of curvature $\kappa$ can be suggested as

$$\kappa < 586/2\mathscr{R}^2.$$

For $\mathscr{R} > 200$, as the curvature and torsion are small, the governing equations (6)–(7) can be simplified without loss of accuracy by neglecting the functions $F_1$ and $F_2$ in (6) and (7). Hence, $h$ and $m$ can be approximated as 1, except that the coefficients of $w_h(\partial w_h/\partial r)$ and $w_h(\partial w_h/\partial\theta)$ are replaced by $2\kappa\sin\theta$ and $2(\kappa\cos\theta-\tau^2 r)/r$, respectively. As a result, (6) and (7) are simplified as

$$\nabla^4\psi_d - \frac{1}{r}\frac{\partial(\psi_d, \nabla^2\psi_d)}{\partial(r,\theta)} = -Kw_d\left(\sin\theta\frac{\partial w_d}{\partial r} + \frac{\cos\theta}{r}\frac{\partial w_d}{\partial\theta}\right) + Tn\left(\frac{1}{r}\frac{\partial(\psi_d, w_d)}{\partial(r,\theta)} - \nabla^2 w_d + 4\right) + \tfrac{1}{2}Tn^2 w_d\frac{\partial w_d}{\partial\theta}, \quad (26)$$

and

$$\nabla^2 w_d - \frac{1}{r}\frac{\partial(\psi_d, w_d)}{\partial(r,\theta)} + 4 = 0, \quad (27)$$

where the parameters $w_d$ and $\psi_d$ used by Dean (1928) for the loosely coiled pipe are

$$w_d = \frac{w_h}{\mathscr{R}}, \quad \psi_d = -\psi. \quad (28)$$

From (27), (26) can be further expressed as

$$\nabla^4\psi_d - \frac{1}{r}\frac{\partial(\psi_d, \nabla^2\psi_d)}{\partial(r,\theta)} = -Kw_d\left(\sin\theta\frac{\partial w_d}{\partial r} + \frac{\cos\theta}{r}\frac{\partial w_d}{\partial\theta}\right) + 8Tn + \tfrac{1}{4}Tn^2\frac{\partial w_d^2}{\partial\theta} \quad (29)$$

which is exactly the same as the extended Dean equations of Germano (1989) for small curvature $\kappa$ and torsion $\tau$ if the following transformations are made:

$$Tn = K\lambda/\mathscr{R}, \quad \xi = \theta + \tfrac{1}{2}\pi,$$

where $\lambda = \tau/\kappa$ and $\xi$ is the polar angle used by Germano (1989). Consequently, the flow rate solution of the extended Dean equations of Germano (1989) ((27) and (29)) which has not been solved yet is simply (25).

The expanded series equations for (26) and (27) can be obtained from (17) and (18) by neglecting the $H_{ij}^{(1)}$ and $H_{ij}^{(2)}$ terms. With appropriate transformations as stated in (28), the series solutions of $w_d$ and $\psi_d$ are the terms with the highest power of $\partial p/\partial s$ in $w_{ij}$ and $\psi_{ij}$ of (20) and (21), respectively.

Although the approaches of Germano (1989) and the present work are different, both reach the same extended Dean equations. Based on the non-orthogonal coordinate system and the stream function defined, without using any coordinate transformation (Germano 1989), the present derivation is more general. The pseudo-stream function defined by Germano (1989) is shown to be a special case of (5) devised in the present work.

To study the torsion effect, Germano (1989) introduced a parameter $\lambda/\mathscr{R}$ to estimate the relative effect of torsion and curvature. However, the torsion number $Tn$ as defined in this work can be employed to estimate purely the torsion effect. A similar parameter $T = \tau\mathscr{R}$ has been also reported by Germano (1989) for a twisted

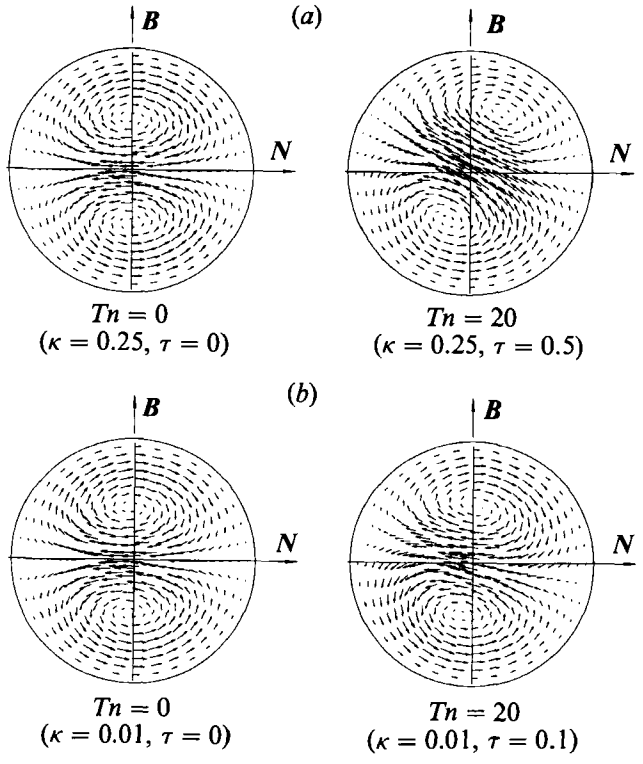


FIGURE 6. The influence of the torsion number $Tn$ on the secondary flow patterns: (*a*) $\mathscr{R} = 20$, $K = 200$; (*b*) $\mathscr{R} = 100$, $K = 200$.

pipe with elliptical cross-section. It seems to be reasonable to state that the presently defined torsion number $Tn$ could be further used to estimate the torsion effect of helical or twisted pipes with different cross-sections.

### 5.2. *Secondary flow patterns*

To explore the torsion effect on the secondary flow patterns, the velocities $(u, v, w)$ in a non-orthogonal helical coordinate system $(r, \theta, s)$ can be rewritten in an orthogonal coordinate system $(r, \theta, s')$ used by Kao (1987) as follows:

$$u' = u, \quad v' = v + \tau r w_h, \quad w' = (2\kappa)^{\frac{1}{2}} m w_h. \tag{30}$$

The velocity components $(u', v', w')$ are defined with respect to coordinates $(r, \theta, s')$ accordingly. The secondary flow pattern composed of the projected velocity vectors $(u', v')$ can be visualized directly from experiment. The major difference between the non-orthogonal helical coordinate system $(r, \theta, s)$ and the orthogonal one $(r, \theta, s')$ is at the axes $s$ and $s'$. The $s$-axis is not perpendicular to the $(r, \theta)$-plane except at the centre point of the $(r, \theta)$-plane. However, the $s'$-axis is always perpendicular to the $(r, \theta)$-plane and its direction coincides with that of the tangential vector $\boldsymbol{T}$ of the centreline. The relations between $(r, \theta, s)$ and $(r, \theta, s')$ coordinates are shown in figure 3.

Figure 6 shows the influence of the torsion number $Tn$ on the projected-velocity vectors $(u', v')$ (secondary flow) under different Reynolds numbers $\mathscr{R}$. For $\mathscr{R} = 20$, a pair of symmetrical vortices occurs when $Tn = 0$ and the vortices are twisted clockwise significantly when $Tn = 20$. Since the cross-section of helical pipes is

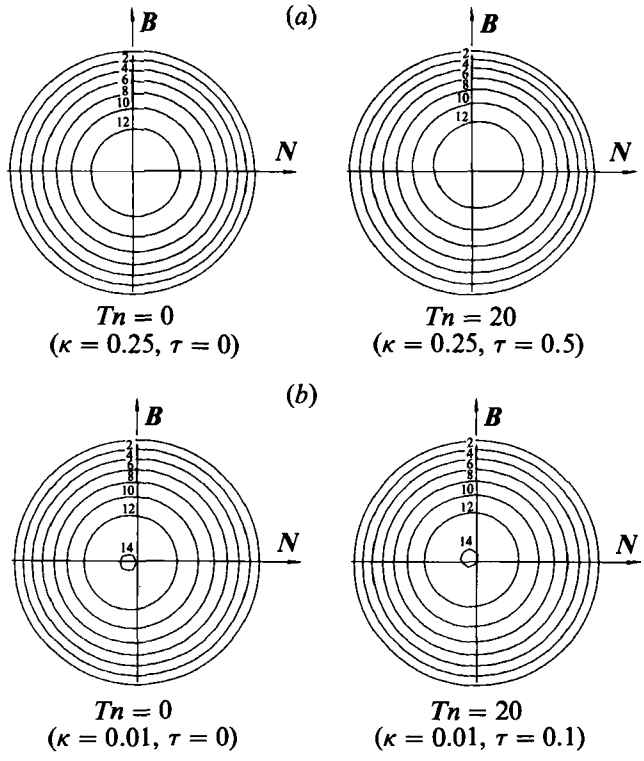


FIGURE 7. The influence of the torsion number $Tn$ on the axial velocity contour: (*a*) $\mathscr{R} = 20$, $K = 200$; (*b*) $\mathscr{R} = 100$, $K = 200$.

twisted counterclockwise as seen in figure 2, the twisting force rotates the vortices clockwise. The degree of tendency also depends on $\mathscr{R}$, which represents the inertial force of the flow, and torsion $\tau$, which represents the change of the geometry of the helical pipe. As $\mathscr{R}$ increases and $K$ and $Tn$ remain constant, the torsion effect becomes more insignificant.

Kao (1987) observed that torsion can produce a large effect on the secondary flow if the ratio of the curvature to the torsion is of order unity. Although this is not shown quantitatively in figure 6, from the solution of stream function (15) it can be expected that the torsion effect on the secondary flow is enhanced as curvature increases. A similar phenomenon is also observed on the flow rate.

### 5.3. *Axial velocity contours*

The torsion swirls the flow about the centre of the cross-section of the pipe. Hence, the torsion effect on the axial velocity can be observed only when the axial velocity contour is off-centre or not axisymmetrical. That is, for a helical circular pipe, the influence of torsion exists only when the centrifugal force acts. This is also consistent with the flow rate equation (24). If $K$ vanishes, no matter how large $Tn$ is, the flow rate always equals 1.

The contours of the axial velocity $w'$ for cases corresponding to figure 6 are shown in figure 7. For $\mathscr{R} = 20$, although $K$ is high, up to $K = 200$, it is interesting to note that the contour of the axial velocity shifts slightly towards the inner wall of the pipe when $Tn = 0$. This phenomenon, similar to that observed by Larrain & Bonilla (1970) for a toroidal pipe can be also explained by the superposition of the present

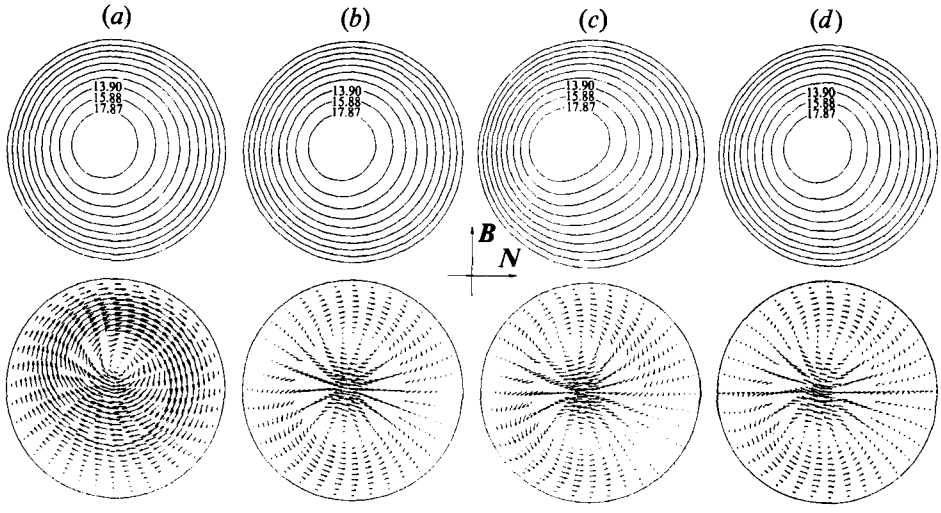


FIGURE 8. The flow patterns of the present and Kao's problem. (*a*) Present solution in non-orthogonal coordinate system. (*b*) Present solution in an orthogonal coordinate system. (*c*) Kao's series expansion solution. (*d*) Kao's numerical solution ($\mathscr{R} = 200$, $K = 400$ and $Tn = 20$).

series solutions $w_{10}$, $w_{20}$, $w_{30}$ and $w_{40}$. As $Tn$ increases to 20, the contours of the axial velocity are shifted to the upper-right region, which agrees with that of Kao's numerical solutions. As $\mathscr{R}$ increases to 100, as would be expected, both the curvature and torsion effects on the axial velocity contours are not so obvious.

### 5.4. *Solutions of Kao's problem*

The solutions of the velocity components computed by the different coordinate systems used by Kao (1987) and in the present work can be further studied in figure 8. Figures 8(*a*) and 8(*b*) show the present results computed by the double series expansion method. They are expressed in the non-orthogonal coordinate system used by Wang (1981) and the present work and in the orthogonal coordinate system used by Germano (1982, 1989) and Kao (1987). For a consistent comparison, the axial velocity in figure 8(*a*) has been multiplied by a factor $(2\kappa)^{\frac{1}{2}}$ to make the same scale as $w'$, and the projected velocity vectors in figure 8(*a*) and 8(*b*) have also been adjusted to the same scale as those of Kao (1987).

To see the difference between the computations based on different coordinate systems, it is better to start with the axial velocity $w$ and its components. As seen in figure 3, the axial velocity $w$ of the non-orthogonal coordinate system $(r, \theta, s)$ can be divided into two components, say, $mw_h$ and $\tau r w_h$. The component $mw_h$ which is directed perpendicularly to the $(r, \theta)$-plane is simply the axial velocity $w'/(2\kappa)^{\frac{1}{2}}$ defined in the orthogonal coordinate system $(r, \theta, s')$ (Germano 1982, 1989; Kao 1987). For the cases studied in figure 8, since the curvature and torsion are small ($\kappa = 0.005$ and $\tau = 0.05$), $mw_h$ is nearly the same as $w$ and the difference between the axial velocity contours of figures 8(*a*) and 8(*b*) is negligible.

The component $\tau r w_h$ on the $(r, \theta)$-plane plays the role of part of the angular velocity $v'$. Because the axial velocity $w$ is much larger than the velocities $u$ and $v$, the component $\tau r w_h$ has a profound influence on the calculation of the angular velocity $v'$ and the secondary flow as seen in figures 8(*a*) and 8(*b*). The secondary flow expressed in the non-orthogonal coordinate system $(r, \theta, s)$ (figure 8*a*) shows a single strong vortex which rotates clockwise. Wang (1981) observed this and stated that

the torsion produces a first-order effect. However, after adding the counterclockwise angular velocity component $\tau r w_h$ onto the projected velocity vectors $(u, v)$ to compose the secondary flow in the orthogonal coordinate system $(r, \theta, s')$ (figure 8*b*), a pair of weak vortices occurs and, as mentioned by Germano (1982), the torsion effect on the secondary flow is only of second order. The inconsistency of the torsion effect on the secondary flow between Wang (1981) and Germano (1982) due to the different coordinate systems used is thus quantitatively explained. This also confirms the qualitative description of Tuttle (1990).

Figures 8(*c*) and 8(*d*) are Kao's (1987) results obtained by a single series expansion method and numerical method, respectively. The axial velocity contours of $w'$ and the secondary flow in figure 8(*d*) by a numerical method are nearly the same as those in figure 8(*b*) obtained by the present study. Since Kao (1987) expanded the series only with $K$, the results of figure 8(*d*) should be reasonable as compared with those of figure 8(*c*).

## 6. Conclusions

Using the exact flow solution derived for a twisted circular pipe, the solution for a helical circular pipe has been successfully obtained by the double series expansion method. Since the high-order terms of the curvature $\kappa$ and torsion $\tau$ are considered in the governing equations, the solutions are also applicable to cases with finite curvature $\kappa$ and finite torsion $\tau$. Because the governing equations and series solutions for each expansion order are written in compact forms, the complete series solution can be computed by a systematic procedure on computer.

From the flow rate equation, it is concluded that the flow in a helical pipe is governed by three parameters: Reynolds number $\mathscr{R}$, Dean number $K$ and torsion number $Tn$. The torsion number, $Tn = 2\tau\mathscr{R}$, induced by the torsion makes the flow different from that in a toroidal pipe. In general, an increase of $K$ decreases the flow rate and enhances the torsion effect on the flow. The variation of $Tn$ has a significant effect on the flow rate and the secondary flow, especially when $\mathscr{R}$ is small. For a helical circular pipe, the torsion effect makes the flow rotate in a direction opposite to the torsion. In addition, the influence of torsion depends on the cross-section geometry of the helical pipe.

When $\mathscr{R} > 200$ and curvature and torsion are small, the general governing equations are reduced to the extended Dean equations for a helical pipe as stated by Germano (1989), which are dominated by $K$ and $Tn$ only. The flow rate solution of the extended Dean equations is also presented. The inconsistency of the torsion effect on the secondary flow between Wang (1981) and Germano (1982, 1989) can be quantitatively explained by the different coordinate systems used.

With the achievements of the present work, the approach can be further extended to deal with the fully developed forced-convective heat transfer to viscous flow in a helical circular pipe especially for cases with finite curvature and finite torsion. This will be given in a subsequent report.

The authors are grateful to the National Science Council of the Republic of China for the financial support through grant NSC80-0401-E007-29.

## REFERENCES


BERGER, S. A., TALBOT, L. & YAO, L. S. 1983 Flow in curved pipes. *Ann. Rev. Fluid Mech.* **15**, 461.

CHEN, W. H. & FAN, C. F. 1986 Finite element analysis of incompressible viscous flow in a helical pipe. *Comput. Mech.* **1**, 281.

DEAN, W. R. 1928 The stream-line motion of fluid in a curved pipe. *Phil. Mag.* **5**, 673.

GERMANO, M. 1982 On the effect of torsion on a helical pipe flow. *J. Fluid Mech.* **125**, 1.

GERMANO, M. 1989 The Dean equations extended to a helical pipe flow. *J. Fluid Mech.* **203**, 289.

ITŌ, H. 1987 Flow in curved pipes. *JSME Intl J.* **30** (262), 543.

KAO, H. C. 1987 Torsion effect on fully developed flow in a helical pipe. *J. Fluid Mech.* **184**, 335.

KOTORYNSKI, W. P. 1986 Steady laminar flow through a twisted pipe of elliptical cross-section. *Computers Fluids* **14**, 433.

LARRAIN, J. & BONILLA, C. F. 1970 Theoretical analysis of pressure drop in the laminar flow of fluid in a coiled pipe. *Trans. Soc. Rheol.* **14**, 135–147.

MANLAPAZ, R. L. & CHURCHILL, S. W. 1980 Fully developed laminar flow in a helically coiled tube of finite pitch. *Chem. Engng Commun.* **7**, 57.

MURATA, S., MIYAKE, Y., INABA, T. & OGAWA, H. 1981 Laminar flow in a helically coiled pipe. *Bull. JSME* **24**, 355.

TODD, L. 1977 Some comments on steady, laminar flow through twisted pipes. *J. Engng Maths* **11**, 29.

TOPAKOGLU, H. C. 1967 Steady laminar flows of an incompressible viscous fluid in curved pipes. *J. Math. Mech.* **16**, 1321.

TUTTLE, E. R. 1990 Laminar flow in twisted pipes. *J. Fluid Mech.* **219**, 545.

VAN DYKE, M. 1978 Extended Stokes series: laminar flow through a loosely coiled pipe. *J. Fluid Mech.* **86**, 129.

WANG, C. Y. 1981 On the low-Reynolds-number flow in a helical pipe. *J. Fluid Mech.* **108**, 185.

XIE, D. G. 1990 Torsion effect on secondary flow in a helical pipe. *Intl J. Heat Fluid Flow* **11**, 114.